Materials Science-Poland, Vol. 23, No. 1, 2005

Formation of nanostructures with a controlled size distribution in Si-based gels by ion irradiation

JEAN-CLAUDE PIVIN*

C.S.N.S.M., Bâtiment 108, 91405 Orsay Campus, France

Studies of irradiation effects in inorganic polymers and gels performed at CSNSM during the past 10 years are overviewed and examples of precipitations with interesting applications (C, Si, metals) occurring during the conversion into ceramics are presented. The precipitation yield, as a function of irradiation fluence or annealing conditions, and particle physical properties were investigated by means of various techniques, depending on their nature. The rates of gel-to-ceramics conversion and of precipitation are determined by the density of electronic excitations produced by ion irradiation (collision cascades slightly assisting the diffusion of metal atoms). Particles formed by ion irradiation show a narrower range of sizes and consequently more interesting characteristics for magnetic or optical applications than those formed in heat-treated gels.

Key words: *sol-gel; nanomaterial; ion irradiation*

1. Introduction

Materials with nanometric structures not only have technological applications in various areas, but also are of fundamental interest for studying the changes of phase properties in this transition regime between the bulk and molecular scales. Sol-gel chemistry is a very convenient technique for producing nanomaterials with a wide range of compositions. The rate of reactions occurring during their thermal processing and the evolution of some components are, however, not well controlled. The ceramics obtained are often porous, heavily cracked, and the particles of the secondary nanophase tend to exhibit a wide range of sizes.

Studies of irradiation effects in inorganic polymers and gels performed during the past 10 years have demonstrated the interest in using this route instead of thermal processing for releasing only hydrogen and obtaining ceramic films fully densified and free of cracks (they are principally due to a mismatch in the expansion coeffi-

*E-mail: pivin@csnsm.in2p3.fr.

cients of the film and substrate in the case of heat treatments) [1]. The out-of-equilibrium nature of ion irradiation chemistry also permits selective promotion of some reactions between gel components, because the formed radicals are able to migrate only at short range, among other reasons. This paper reports the control of the size of various types of particles formed in Si-based gels under ion irradiation and their optical or magnetic properties. The first type of precipitation studied is that of C or Si atoms in excess with respect to the equilibrium composition of glasses, $SiO_xC_{1-x/2}$ (with $1- x/2 \leq 1/4$). The second is the precipitation of transition metals in gels from triethoxysilane (hereafter labelled TH). Different physical quantities are used to assess the precipitation kinetics as a function of the fluence and mass of ions, depending on the nature of the particles.

2. Experimental

Silicon ethoxides (TEOS, MTES, PTES, and mixtures of these precursors) were hydrolysed as usual by adding 2 moles of water and 10^{-2} moles of nitric acid for each mole of ethoxide in ethanolic solution and stirring for 1 h at room temperature, after which films with a thickness of 400–500 nm were deposited by spinning the filtered gel on Si wafers. Triethoxysilane mixed in equimolar proportion with pure ethanol was simply stirred for 5 min before adding salts of various metals M (M = Fe, Co, Ni, Cu). The TH:M filtered gels were used immediately for spinning films, in order to hamper the progressive hydrolysis of Si–H bonds and their possible reaction with metal ions before treatment (noticed only in the case of Cu^{2+}). Analyses of films without salt, by means of ion beam techniques, show that a silicon suboxide $SiO_{1.5}$ containing less than 2 at. % C is obtained with this simple procedure, followed by irradiation or heat treatment for removing H. The O/Si content increases a little (up to 1.7 times) in films from sols containing 10–20 mol % $MNO_3{\cdot}xH_2O$ (M=Fe, Ni, Co) or 20 % $CuCl_2{\cdot}2H_2O$ (the addition of $CuNO_3$ catalyses the precipitation of silica).

Ions of various masses and energies in the MeV range were used for varying the yields of electronic excitations and atomic displacements in the films. The electronic and nuclear stopping powers, S_e and S_n, of 3 MeV Au ions are of same order of magnitude (1.5 and 3.0 keV/nm, respectively), and the total S_e value obtained by adding the energy lost by recoil atoms and primary ions becomesequals to S_n. Si ions of 3 MeV were selected for producing a comparable linear density of electronic excitations (S_e = 1.8 keV/nm) and much smaller atomic displacements (S_n = 100eV/nm). 1 MeV He ions also lose their energy essentially in electronic excitations with a lower density of 300 eV/nm. Ag ions of 100 MeV were also used in a limited number of experiments for increasing the S_e value up to 20 keV/nm while keeping S_n at a low level of 300 eV/nm. Note finally that all these ions stop at some micrometers in the substrate.

The composition of films was analysed by means of ion beam techniques: (i) by Rutherford Back-scattering Spectrometry (RBS), with 2.4 MeV He at normal incidence, for studying the depth profiles of heavy elements; (ii) by Elastic Recoil Detec-

tion Analysis (ERDA), with 3 MeV He ions for profiling H, and (iii) by $^{16}O(d, p)^{17}O$ and $^{12}C(d, p)^{13}C$ Nuclear Reactions Analysis (NRA), with deutons of 920 keV, for determining the areal densities of these elements more accurately than with RBS. Their structure was studied by X-ray diffraction at grazing incidence and TEM observations of cross-sections, prepared by mechanical polishing followed by ion etching. Nanochemical investigations were carried out on TEM samples containing C clusters, using a high resolution Philips CM 20 FEG field emission electron microscope, run at 200 kV and equipped with a Gatan Imaging Filter (GIF 200). Besides electron energy loss spectroscopy at an energy resolution of 0.8 to 1 eV, this filter enables a specific element to be imaged with a spatial resolution better than 1 nm (energy filtered electron microscopy, EFTEM). Optical transmittance spectra in the wavelength range 200–800 nm were recorded with a CARY 5 VARIAN UV-VIS-NIR dual beam spectrometer. The formation of C and Si nanoparticles was characterized by measuring photoluminescence (PL) in the visible range, with excitation by a 488 nm line Ar^+ ion laser at a power density below 1 W/cm^2, and analysing the emitted light by a double SPEX 1403 monochromator and an EMI 9863B photomultiplier. Electron spin resonance (ESR), with a Bruker spectrometer operating at 9.8 GHz (X-band) and equipped with 100 kHz modulation, was used for studying the precipitation kinetics of the magnetic phases and the magnetization anisotropy of the films at room temperature (RT). In addition, measurements of magnetization were performed as a function of the applied field H and temperature T with a SQUID magnetometer S600X from Cryogenic Ltd.

3. Study of H radiolysis and C or Si precipitation

Typical kinetics of hydrogen (H) evolution from Si-based gels with different C contents are presented in Figure 1, for example under He irradiation. The variation in H concentration is plotted versus the integrated amount of electronic excitations, $S_e\phi$, where ϕ is the ion fluence (ions/cm^2), because a comparison of the various ions effects shows that S_n plays no significant role in the process. A detailed analysis of the kinetics shows that the release of H_2 molecules obeys an exponential law (the retained H concentration varies as $\exp(-\sigma S_e \phi)$) up to a given fluence. Above this fluence, the radiolytic efficiency σ decreases and the evolution kinetics is limited by the combination rate of H radicals inside ion tracks to form molecules [2]. The σ value decreases markedly with increasing C content in the material, whose effect is attributed to the strength of C–H bonds with respect to O–H bonds (this strength also increases as CH_3 groups are partially decomposed).

Energy-filtered TEM images of the C distribution in cross-sections of the irradiated films provides evidence that C atoms or CH_x radicals migrate in the structure to form clusters with a diameter of 3–7 nm, depending on the C content and irradiation conditions (S_e value). In the case of phenyl-substituted precursors (PTES and silsesquioxanes), clusters are also supposed to form on the spot of the radiolysis event [1].

Ions with a low energy per nucleon, such as 3 MeV Au ions, are scattered in random directions during nuclear collisions, while swift ions undergoing only electronic stopping have a straight path.

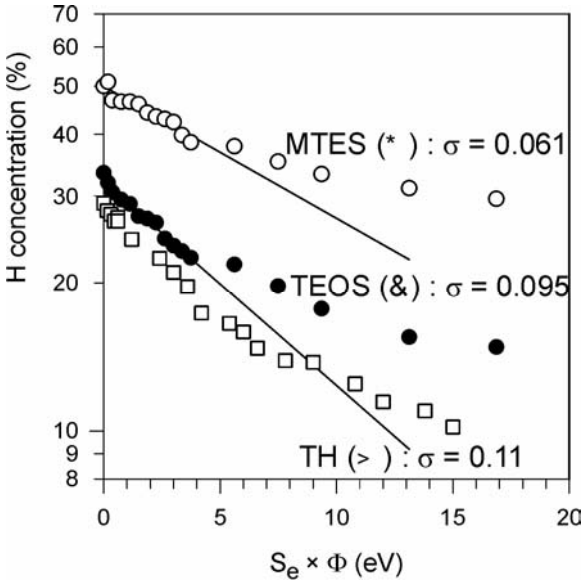

Fig. 1. Kinetics of H release in various gels (TEOS, TH, MTES) under He irradiation and a fit of the initial decrease of H concentration ρ with the simple exponential law $\rho = \rho_0 \exp(-\sigma S_e \phi)$

Accordingly, one observes C clusters with a random or a linear distribution along ion tracks, as shown in Figure 2. It is known that regions with a perturbed structure in swift ion tracks may be spherical and isolated, oblong, or percolating in the form of cylinders, depending on S_e and on ion velocity [53]. The last geometry mentioned seems to be obtained in the case of 100 MeV Ag irradiation of MTES films, and this result may find applications in fabricating field-emitting fibres or electric contacts with a well defined and very small section. Whatever the shape of the C particles, Raman scattering analyses show that they exhibit a noticeable degree of tetragonal hybridisation [1]. These semiconducting particles emit a yellow-green luminescence, with a maximum yield for a defined amount of excitations $S_e\phi$ of 30 eV$\times 10^{23}$ ions/cm^3 [4]. The PL emission wavelength and intensity seem to be the same for spherical clusters and cylinders obtained for a given $S_e\phi$ value [5]. On the other hand, the peak position shifts from 460 to 540 nm with irradiation fluence as the clusters grow under the cumulative effects of ions in same spot. It is worth noting that films of same nature annealed at 1000 °C in a vacuum of 10^{-7} torr (for not burning C) exhibit no excitonic luminescence [5]. Raman analyses indicate that this is due to the graphitic nature of the clusters [6]. The difference in the hybridisation states of annealed and irradiated films can be ascribed either to the known formation of sp^2 rings upon a critical cluster size or to a tendency towards a more stable structure during annealing treatment [1, 6].

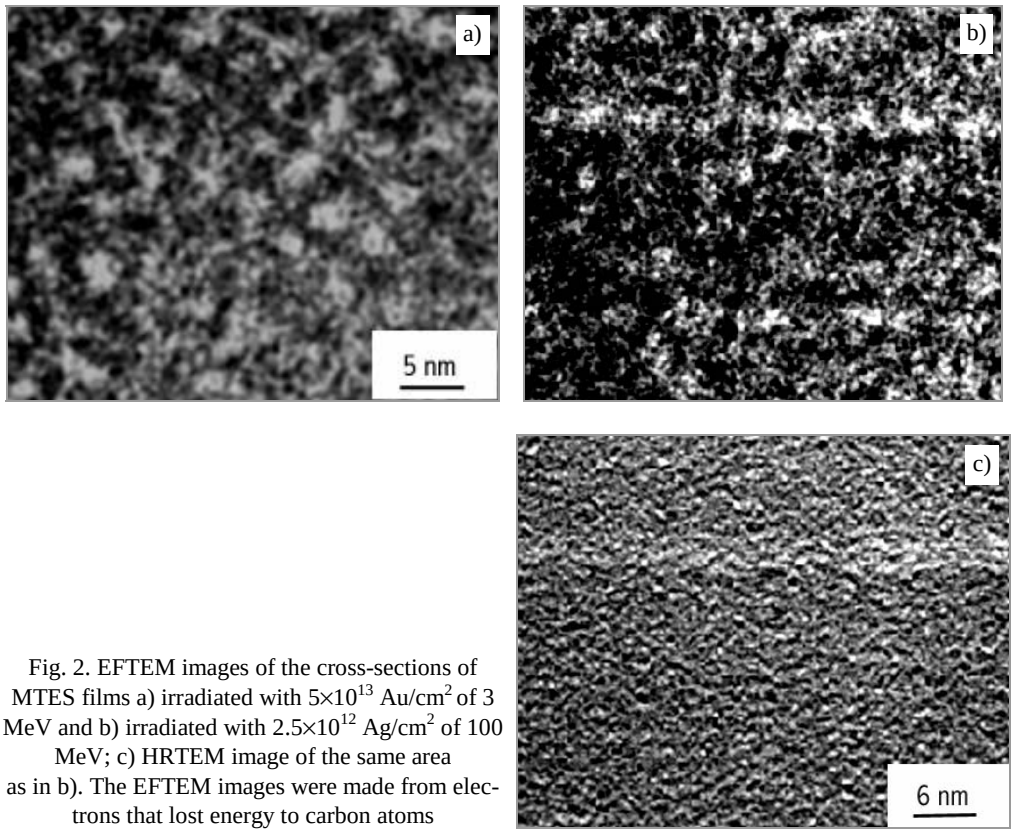

Fig. 2. EFTEM images of the cross-sections of MTES films a) irradiated with 5×10^{13} Au/cm^2 of 3 MeV and b) irradiated with 2.5×10^{12} Ag/cm^2 of 100 MeV; c) HRTEM image of the same area as in b). The EFTEM images were made from electrons that lost energy to carbon atoms

Similarly to C in MTES, PTES and silsesquioxanes, Si precipitates under irradiation in Si suboxide derived from TH, and the semiconducting clusters show a red luminescence with a wavelength correlated to the particle size (~1 nm) [7]. In the case of TH films, the small departure from SiO_2 stoichiometry makes particles formed during annealing treatments at 1000–1100 °C in vacuum have an optimum size of 2–3 nm for the luminescence of confined excitons [8].

4. Studies of metallic precipitations in TH

Precipitations of Cu, Fe, Co, and Ni are observed by means of TEM in samples containing 10 to 25 mol % of salt and irradiated with 3 MeV Au ion fluences of 5×10^{14} to 10^{15}/cm^2 [9]. Their range of size is relatively narrow (the distribution is of a gaussian type with a standard deviation/mean size ratio of 25%) and their spatial distribution is homogeneous. On the contrary, the size distribution of particles formed in films heat-treated at 600 °C in vacuum is of the lognormal type with a half-width/mean size ratio of 100%. In addition, ovoid porosities are systematically ob-

served in annealed TH:Ni and TH:Co samples, and the particles are segregated on pore walls and on some linear defects (which may be nanocracks, see Fig. 3).

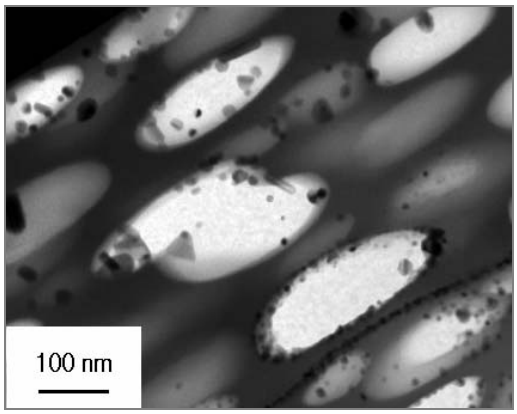

Fig. 3. TEM image of the cross section of a TH Ni film (3 at.% Ni) annealed at 600 °C. The large axes of porosities are parallel to the film surface

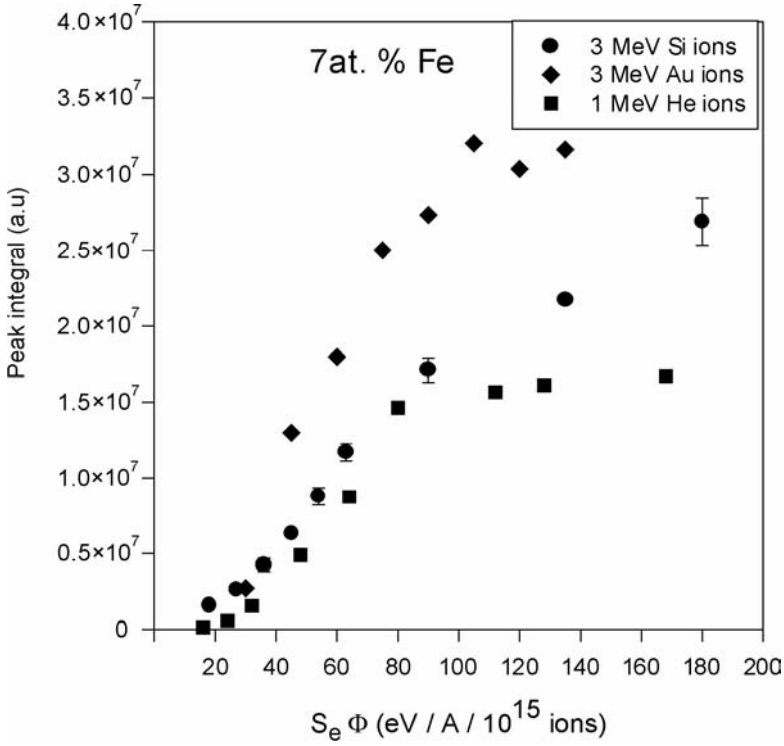

Fig. 4. Variation of the integral of the absorbed power measured in electron spin resonance from TH films doped with 20 mol % $FeNO_3$ (7.5 at. % Fe in the glass) as a function of the energy deposited in electronic excitations under 1 MeV He, 3 MeV Si, and 3 MeV Au irradiation

X-ray diffraction spectra show that silicides form when the annealing temperature reaches 1000 °C. The formation of a ferromagnetic phase is detected by means of ESR for a threshold energy $S_e\phi$ of 40 eV×10^{23} ions/cm^3. The total volume V of the magnetic phase, estimated from the integral of absorbed power seems to obey the law typical of precipitation processes under irradiation for ions producing few displacements ($1 - \exp(-\sigma S_e \phi)$), and to be linear function of the fluence under 3 MeV Au irradiation (Fig. 4). The rates V/S_e are, however, very close for the various types of ions. The different behaviour of Au irradiated films is ascribed to the occurrence of radiation-induced diffusion on short range, assisting the segregation of metal atoms. A similar change of kinetic law was observed previously for the formation of amorphous clusters in metallic alloys, according to the irradiation temperature [10]. Another effect of displacements, which can be observed in Fig. 4, is the occurrence of a magnetization maximum of the order of 8×10^{14}/cm^2 for a fluence of 3 MeV Au ions. It is interpreted to be due to a re-dissolution of the clusters by cascade mixing. This dissolution is confirmed by the observation of a linear decrease in magnetization when submitting pre-annealed samples to irradiation [11]. A study of the resonance peak position, H_{res}, as a function of the direction φ of the applied static field with respect to the surface, shows that the internal field H_i is that of an homogenous ferromagnetic medium, which is given by the Kittel equation:

$$\frac{\omega_0^2}{\gamma^2} = H_0^2 = (H_{res} - H_i \cos 2\varphi) \times (H_{res} + H_i \sin^2 \varphi)$$

where ω_0 is the angular frequency of the cavity and γ the gyromagnetic ratio of the ferromagnetic electrons. H_i is equal to the demagnetising (Zeeman) field H_d when there is no other anisotropy factor than the sample shape and H_d is $-4\pi M$ for a thin plate or $2\pi M$ for a rod, M being the magnetization at saturation of the bulk metal multiplied by the volume fraction f of the metal. Annealed films behave as homogeneous plates, despite the porosities and segregation of particles on defects. The angular variation of H_{res} is of same type in irradiated samples (Fig. 5), but H_i exceeds $-4\pi M$ when the effective precipitation yield f is taken into account. An interesting change in anisotropy is observed when submitting pre-annealed samples to irradiation with swift ions producing cylindrical tracks: the film anisotropy becomes similar to that of an assembly of rods, with the internal field H_i exactly equal to $2\pi M$ (Fig. 5).

In fact, the apparent excess of magnetization in pristine films directly submitted to irradiation ($H_a = |H_i| - 4\pi M$) and maybe also the tilt of the easy magnetization axis in annealed-irradiated films is due to magnetostriction. Nanoparticles of any type undergo a compression, increasing in inverse proportion to their size, under the effect of interfacial energy (Laplace's law), to which the stress induced by the athermal compaction of the matrix and by the limited diffusion of atoms (for accommodating the volume change due to metal precipitation) must be added in the present case. In annealed TH:Ni or TH:Co samples, these stresses are compensated by the formation of voids elongated parallel to the surface (Fig. 3). TEM observations show that the

change in the magnetic anisotropy of annealed films (including TH:Fe films free of voids) after irradiation with high-energy ions is not due to the rearrangement of particles in more or less continuous cylinders and that their size distribution remains the same. Thus, it is ascribed to changes in the stress state related to the creation of defects in the matrix, as already observed for single-phased magnetic materials [3].

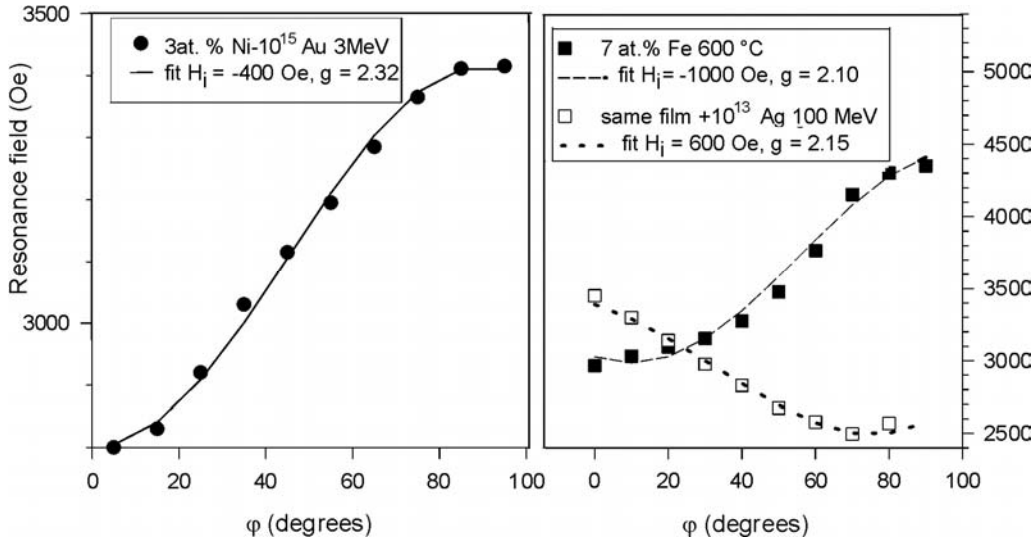

Fig. 5. Anisotropy of spin resonance in TH.M films irradiated with 3 MeV Au, and annealed at 600 °C or annealed then irradiated with 100 MeV Ag ions

There is no place here for a discussion of the superparamagnetic or ferromagnetic behaviour of samples as a function of temperature, metal content, and type of treatment. Interest in the triethoxysilane matrix being a host of metal particles is more worthwhile to emphasize. Films formed from tetraethoxysilane exhibit no magnetisation and X-ray diffraction provides evidence of the formation of antiferromagnetic oxides (annealed samples) or solid solutions (irradiated samples). The formation of fayalite, magnetite, or NiO was observed by other authors in TEOS monoliths that were heat-treated in hydrogen [12]. Irradiation chemistry may also differ noticeably from thermo-chemistry in some cases, since Cu particles with a plasmon resonance in the visible are observed exclusively in TH:Cu irradiated samples [13]. Respectively, the irradiation of TEOS:Ag films or exchanged glasses already containing clusters with very energetic ions (100 MeV Ag or Au) induces a re-dissolution of the clusters [14]. This effect is not yet elucidated nor the absence of detectable precipitation in TH:Fe or TH:Ni pristine films when irradiated with the same ions. Metallic nuclei may explode by Coulombic repulsion between ionised M atoms when the yield of secondary electrons expelled from the track core (always huge) exceeds a threshold value [3].

5. Conclusion

Ion irradiation of gel films leads to the formation of nanoclusters issued from the precursor backbone or from a reaction between precursor side groups and dissolved ions (TH). The driving process is essentially the formation of free radicals via electronic excitations. A defined value of the radiolytic cross section, σS_e, for a given ion species makes clusters exhibit an homogenous size, while they tend to grow by Ostwald ripening in the case of gels converted to ceramics by heat treatment. Changes in the track core dimension ($\pi r^2 = \sigma S_e$) and in the energy of the secondary electrons expelled from the core with increasing velocity of ions [15] seem to induce the gathering of C, Si, or M atoms into narrow cylinders. This new type of nanostructure is of great interest for applications such as magnetic memories perpendicular to the surface, nano-diodes, electric contacts, etc. The density and very good adhesion of irradiated films are also advantages with respect to thermal processing worth keeping in mind whatever the nature of the gel, especially when useful fluences are very low and their cost not prohibitive.

Acknowledgement

Thanks are due to E. Pippel of Max-Planck Institute, Halle, for having performed the EFTEM observations shown in Figure 2.

References

[1] PIVIN J.C., COLOMBO P., SORARU G.D., J. Am. Ceram. Soc., 83 (2000), 713.
[2] SRIVASTAVA S.K., AVASTHI D.K., PIVIN J.C., Nucl. Instr. Meth., B 191 (2002), 7185.
[3] TOULEMONDE M., BOUFFARD S., STUDER F., Nucl. Instr. Meth., B 91 (1994), 108.
[4] PIVIN J.C., SENDOVA-VASSILEVA M., Mater. Sci. Eng., B69 (2000), 574.
[5] KUMAR A., SINGH F., AVASTHI D.K., PIVIN J.C., to be published
[6] PIVIN J.C., COLOMBO P., J. Mat. Sci., 32 (1997), 6163.
[7] PIVIN J.C., COLOMBO P., MARTUCCI A., SORARU G.D., PIPPEL E., SENDOVA-VASSILEVA M., J. , Sol -Gel Sci. Technol., 26 (2003), 251.
[8] JIMENEZ DE CASTRO M., PIVIN J.C., J. Sol-Gel Sci. Technol., 28 (2003), 37
[9] PIVIN J.C., VINCENT E., ESNOUF S., DUBUS M., Eur. Phys. J. B., 37 (2004), 329.
[10] COHEN C., BENYAGOUB A., BERNAS H., CHAUMONT J., THOME L., BERTI M., DRIGO A.V., Phys. Rev., B31 (1985), 5.
[11] PIVIN J.C., ESNOUF S., unpublished results.
[12] ENNAS G., CASULA M.F., FALQUI A., GATTESHI D., MARONGUI G., PICCALUGA G., SANGREGORIO C., PINNA G., J. Non-Cryst. Solids, 293 (2001), 1.
[13] PIVIN J.C., Nuc. Instr. Meth., B216 (2004), 239.
[14] PIVIN J.C., ROGER G., GARCIA M.A., SINGH F., AVASTHI D.K., Nucl. Instr. Meth., B 215 (2004), 373.
[15] CHADDERTON L.T., Rad. Measurements, 36 (2003), 13.

Received 16 July 2004
Revised 25 July 2004